T.5: Advanced and compact laser plasma electron accelerators and its applications

D. Hazra[1] and A. Moorti[2]
[1]*Senior Research Fellow, Homi Bhabha National Institute*
[2]*Advanced Plasma Acceleration Section, Laser Plasma Division*
[2]*Email: moorti@rrcat.gov.in*

Abstract

Research and development of advanced electron acceleration techniques providing higher accelerating electric field gradient than the present radio-frequency (rf) based technique is of current interest, and worldwide efforts are being made towards this with an aim to reduce the size and cost of accelerators, and hence to facilitate its wider availability. In this regard, Laser Plasma Accelerator (LPA) is being seen as a promising candidate, which could also be further used for development of compact Laser Synchrotron Radiation Sources using various techniques. At RRCAT, being a centre working on both lasers and accelerators, this laser and plasma based advanced acceleration technique is being pursued intensively. Using high-power (150 TW), ultra-short duration (25-100 fs) Ti:sapphire laser, and gas-jet plasma targets of 4 mm length, acceleration of electrons to >500 MeV energy has been achieved. Suitability of LPA for radiography and radiotherapy applications was also explored. Setting up of a 1 PW Ti:sapphire laser facility is also under progress and could facilitate generation of $\geq$ GeV energy electron beams for various scientific and applied research.

1. Introduction

Charged particle (electron/proton/ion) accelerators have found several potential applications in various applied and research fields viz. industrial, medical, nuclear and particle physics studies etc. [1], and has shown immense progress over the years. The currently used rf acceleration technique suffers from limited acceleration gradients of ~50 MV/m, leading to large accelerator size and huge costs, forcing the scientific community to explore alternate acceleration techniques providing comparatively higher acceleration gradients. In this regard, various advanced acceleration techniques are being investigated, many involving ultra-short intense laser pulses. Among these, Laser Plasma Accelerator (LPA), based on intense ultra-short laser plasma interaction, has been found to be promising. Plasma being in the broken state has the advantage of sustaining very high accelerating electric field gradients of > 100 GV/m [2,3], thereby could facilitate development of comparatively compact and cheap accelerators.

The unique advantage of LPA is the generation of ultra-short duration electron bunches of the order of femtosecond which could further be used for generation of ultra-short x-ray/γ-ray radiations. While being accelerated, relativistic electrons make betatron oscillations in the plasma channel (in transverse channel as well as laser electric field) leading to emission of synchrotron like radiation known as betatron radiation. Intense, tunable, x-ray/γ-ray radiation could also be generated through inverse Compton scattering process using ultra-short electron bunches generated through LPA. Alternatively, using a magnetic undulator and LPA, compact Free Electron Laser (FEL) could also be set up. Hence, using LPA, so called Laser Synchrotron Radiation Sources could also be developed using the above described techniques. LPA has also been considered for various other possible applications of relativistic electron beams e.g. electron beam radiography and radiotherapy.

LPA is associated with highly non-linear and complex laser-plasma interaction processes [4]. Electron beam generation in various parametric regimes were explored to investigate underlying acceleration mechanisms viz. Laser Wakefield Acceleration (LWFA) [5], Direct Laser Acceleration (DLA) [6] and hybrid acceleration mechanism (LWFA+DLA) [7]. The primary emphasis of the initial investigations was to achieve higher and higher electron energy and also to have a control on the accelerator performance leading to the generation of stable, high-quality electron beams. Generation of quasi-monoenergetic electron beams of sub-GeV to multi-GeV energy accelerated by wakefield has been studied extensively with TW-PW laser systems [2,3] demonstrating maximum energy of ~8 GeV [8]. On the other hand, electron acceleration through DLA mechanism is sparsely studied [9].

At RRCAT, being a centre working on both, lasers and accelerators, this vital area of research and development is being intensively pursued [10,11,12]. Initial experimental studies on LPA were carried out using 10 TW, 45 fs Ti:sapphire laser system providing focused intensity of $> 10^{18}$ W/cm^2. Through interaction with plasma of density in the range of 1-10x10^{19} cm^{-3}, generation of high quality, stable, quasi-monoenergetic electron beams with energy of 20-50 MeV were demonstrated in He [13,14] and also in N_2 gas-jet target of 1.2 mm length [15], and also from plasma plume target with peak energy of 12 MeV [16].

In this theme article, we present our recent investigations on LPA in underdense gas-jet plasma using 150 TW Ti:sapphire laser system with emphasis on determining role of different acceleration mechanisms in generating high-energy electron beams, and also exploring its applications. Experiments were performed with laser pulse durations in the range of ~25-200 fs in different gas-jet plasma targets e.g. He, mixed

gas-jet targets of He+N_2, N_2 and Ar with plasma density in the range of ~10^{18}-10^{20} cm^{-3}. A pure DLA regime of acceleration was identified with long laser pulse duration of 200 fs in He gas-jet target [17] and most interestingly, also with short laser pulse duration of 55-60 fs in high Z gas target of N_2 and mixed gas target of N_2 and He [18,19]. Generation of quasi-monoenergetic electron beams (energy spread ~21%) with peak energy of ~168 MeV accelerated through DLA were demonstrated [19]. Hybrid regime of acceleration was also identified with He gas-jet target where an enhancement of electron energy to >500 MeV was observed [20]. Further, application of relativistic electron beams generated from LPA was also explored and electron-beam radiography of metallic and biological plant samples was performed demonstrating suitability of LPA for radiography, radiotherapy and interrogation purpose [21].

2. Laser plasma accelerator: components and diagnostics

In this section, we discuss the systems and diagnostics requirements for LPA along with basic physical processes associated with it.

2.1 Ultra-short intense laser as a driver

In LPA, an ultra-short, intense laser pulse is used as a driver. Mostly, Ti:sapphire laser system (λ=800 nm), based on chirped pulse amplification (CPA) technique [22], providing few tens to few hundreds of fs duration pulse of extreme peak powers from few terawatt (TW) to petawatt (PW) level is used. The pulse, when focussed to a spot size of few μm to few tens of μm, provides focal intensities of ~10^{18}-10^{19} W/cm^2, i.e. a_0~1-4, where a_0 is the normalized laser vector potential.

2.2 Plasma targets

Various types of plasma targets are used in LPA, such as the supersonic gas-jets (rectangular/circular nozzles), gas-cells, pre-formed plasma channels e.g. in gas-filled capillary discharge etc. Typically, plasma of lengths few mm to several cm have been used. For underdense plasma, various gases e.g. He, N_2, Ar or mixed gases such as He+N_2 are mostly used. Typical plasma density varies in the range of ~$10^{17\text{-}20}$ cm^{-3}.

2.3 Diagnostics

LPA requires precise characterisation of laser and plasma parameters to have controlled operation of the accelerator. Therefore, variety of diagnostics are used for laser parameters measurements e.g. second and third order autocorrelators for laser pulse duration and contrast measurements respectively in the ultra-short regime, laser beam profile and measurement of laser focal spot of size few microns to tens of microns using focal spot imaging setup etc. Plasma electron density is a very sensitive parameter which affects the accelerator performance, and therefore plasma targets are characterised using interferometry technique both for neutral gas density measurement of gas-jet targets, as well as of the plasma channel formed by laser pulse. Stable and long length propagation of laser inside plasma is important for stable, high-quality, high-energy electron beam generation, and therefore several optical diagnostics such as 90° Thomson scattering, shadowgraphy and transmitted laser spectrum are recorded to study the laser plasma interaction. LPA generated electron beam has unique characteristics viz. ultra-short (fs regime) pulse duration, high peak current (kA range), and therefore special electron beam diagnostics are required for its single shot characterization. Phosphor screen imaged on a CCD camera, or image plates (IPs) are used for detecting and recording electron beam profiles. Electron beam charge is estimated using Integrating Current Transformers (ICT) developed for ultra-short electron bunches at CERN, Geneva, by M/s Bergoz, and/or phosphor screens/IPs calibrated using that at conventional accelerator facilities. Suitable magnetic spectrograph is used for measuring electron beam energy and its spectrum [23].

3. Experimental setup and details

Experiments were performed using 150 TW, Ti: sapphire laser system, at Laser Plasma Division, RRCAT, Indore. A photograph of the laser system is shown in Figure T.5.1. The laser operated at a central wavelength of 800 nm, providing a maximum energy of ~3.5 J in a shortest pulse duration of ~25 fs, full-width at half maximum (FWHM).

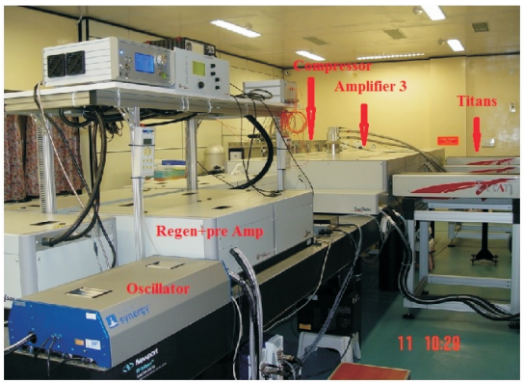

Fig. T.5.1: 150 TW, 25 fs, Ti:sapphire laser system.

Schematic of the experimental set up used for investigations on LPA is shown in Figure T.5.2. During experiment, laser pulse duration was varied from 55 fs to 200 fs and focused to a focal spot of size 6.5-12.5 μm, providing peak laser power of 7.5-20 TW and peak laser intensities of $2x10^{18}$ - $4.3x10^{19}$ W/cm^2 (a_0=1-4.5), on the gas-jet target.

Underdense plasma target of He, mixed (He+N_2), N_2 and Ar gas-jet was used with density in the range of ~10^{18}-10^{20} cm^{-3} using supersonic rectangular gas jet nozzle (length: 1.2 and 4 mm). The gas-jet nozzle was characterized using offline

Mach-Zehnder interferometer for different gas targets. Phosphor screens (DRZ and Lanex) and imaging plates were used to record electron beam profiles. Two types of magnetic spectrographs were used: (i) circular magnet (B~0.45 T, diameter~ 5 cm, pole gap~ 9 mm) for detection of electron in the range of 10-60 MeV with resolution of ~34% at 30 MeV and ~67% at 60 MeV (for 10 mrad beam). (ii) C-shaped rectangular magnet (B~ 0.9 T, dimensions 10×10×20 cm, pole gap~15 mm) to cover a broad energy range of ~15 MeV - 1 GeV, with a resolution of ~8% at 100 MeV and 25% at 300 MeV (for 10 mrad beam) [23]. Electron beam profile and spectra were recorded simultaneously. GEANT4 simulations performed showed negligible loss in electron beam divergence and energy by different components in its path [23]. Laser plasma interaction was studied through 90° Thomson scattering, shadowgraphy and laser forward scattered spectrum.

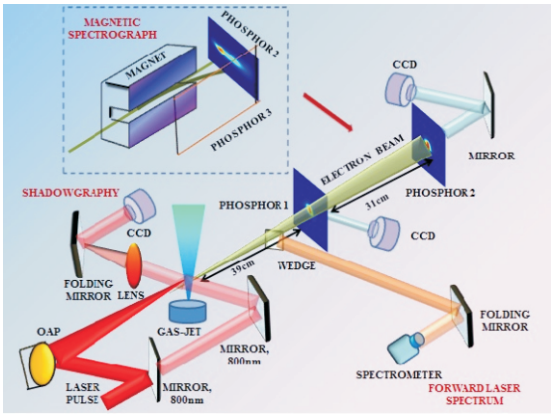

Fig. T.5.2: Schematic of the experimental set up.

4. Laser plasma accelerator: acceleration mechanisms

When intense laser pulse is focused on a gas-jet target, plasma is rapidly created at the foot through tunnel ionization, leading the peak to interact with the plasma. Inside plasma the propagation distance is limited to Rayleigh length $Z_R=\pi r_0^2/\lambda$, (r_0 is initial laser spot radius at $1/e^2$ value of peak intensity and λ is the laser wavelength) due to natural diffraction. It ranges from sub mm to few mm and is not sufficient to accelerate high energy electrons. Laser propagation is also limited by ionization induced defocusing effects, which can be minimized using low Z gas targets such as H_2 and He.

Guiding and propagation of intense laser pulses in underdense plasma beyond Z_R can be achieved through various non-linear processes, such as relativistic self-focusing and ponderomotive channeling, when laser power exceeds critical power for relativistic self-focusing, P_c (GW) = 17.4 x (n_c/n_e), where n_c is the critical density and n_e is the plasma density [24]. Formation of non-linear wakefield (bubble: a region deprived of electrons) and use of preformed density targets [8] helps to guide laser pulse to long distances**.** Various mechanisms of electron acceleration applicable in LPA depending on laser and plasma conditions are described below:

4.1 Laser wakefield acceleration

Most widely investigated scheme in LPA is wakefield acceleration (LWFA) [5], in which intense ultra-short laser pulse excites large amplitude electron plasma wave (wakefield). It moves behind the laser pulse with a phase velocity (v_ϕ) equal to the group velocity (v_g) of the laser in the plasma given by:

$$v_\phi = v_g = c\sqrt{1-\frac{\omega_p^2}{\omega^2}}$$

where c is the speed of light in vacuum, ω is the laser frequency, and ω_p is the plasma frequency given by:

$$\omega_p = \sqrt{n_e e^2/m\varepsilon_0} \approx 5.64\times10^4\sqrt{n_e(cm^{-3})}\,rad/s$$

where m and e are the electron rest mass and charge respectively, and ε_o is permittivity of free space. For $\omega_p<<\omega$, $v_\phi=c$, and hence can be used to accelerate electrons to relativistic energies. The maximum electric field that the plasma wave can sustain is called the cold wave breaking field given by:

$$E_0\ (V/m) = m\omega_p c/e$$

Plasma waves are said to be linear when $E<<E_0$, executing simple sinusoidal oscillation with frequency ω_p. On the other hand, when $a_0>1$ the wave becomes highly non-linear with steepening of density profile and exhibits a sawtooth profile. Efficient excitation of wakefield requires $L\sim\lambda_p$, where $L=c\tau$ is the laser pulse length, τ is the FWHM laser pulse duration and λ_p is the plasma wavelength. For electron densities of ~10^{19} cm^{-3}, this matching requires a laser pulse length of ~30 fs.

Initially, the available laser pulse lengths were much longer to satisfy the resonance condition and plasma beat-wave LWFA was suggested [5]. Later, with comparatively shorter laser pulses of hundreds of fs and several tens of fs duration, $L>>\lambda_p$ and $L>\lambda_p$ regime could be achieved respectively, and Self-Modulated LWFA (SM-LWFA) scheme was proposed. SM-LWFA generally operates at high plasma densities (10^{19} cm^{-3}) and electron beams both with broad continuous ($L>>\lambda_p$) [25], and quasi-monoenergetic spectrum ($L>\lambda_p$) were observed [26] with maximum achievable energy of few tens of MeV. Later, bubble or blow-out scheme of acceleration was proposed [27,28], applicable for the condition of $L<\lambda_p$

regime, with comparatively shorter laser pulse duration of few tens of fs and lower plasma densities of ~$10^{17\text{-}18}$ cm^{-3} fulfilling the matching condition [28]:

$$k_p r_0 = k_p R \cong 2\sqrt{a_0},$$

where $k_p = 2\pi/\lambda_p$. Several investigations in the bubble regime of acceleration demonstrated generation of good quality quasi-monoenergetic sub-GeV to multi-GeV electron beams with the highest achievable energy of 8 GeV [8] and has therefore proved to be a promising technique. Electrons accelerated from LWFA gains maximum energy upto the dephasing length (propagation length up to which electrons remain in the accelerating phase of the plasma wave), beyond which electrons loose energy. This maximum dephasing limited energy gain in the linear [5] and non-linear limit [28] respectively are given by:

$$E_d\,(\text{linear}) = 2(n_c/n_e)\,mc^2$$
$$E_d\,(\text{non-linear}) = 2/3(n_c/n_e)a_0\,mc^2$$

4.2 Direct laser acceleration

In LPA electrons could also gain energy by DLA mechanism [6, 9], in $L>>\lambda_p$ and even $L>\lambda_p$, i.e. when there is significant overlap of laser pulse with the injected electrons. Electrons oscillating at betatron frequency in the self-generated static electric and magnetic fields of the laser created plasma ion channel resonantly gains energy directly from the laser field. DLA is particularly attractive as it can generate high-energy x-ray compared to LWFA due to comparatively higher oscillation amplitude of the electrons. In case of DLA, energy of the accelerated electrons γ with phase ϕ is given by [29]:

$$\frac{d\gamma}{d\phi} = -\frac{eA_0 v_{xA}\cos\phi}{2mc^2\left(\omega - \frac{\omega_{b0}}{\sqrt{\gamma}} - kv_z\right)} \qquad (1)$$

Integrating Eq. (1) we get $F(\gamma) = P\sin\phi + C$, where

$$F(\gamma) = \gamma - \eta\sqrt{(1-\alpha_0)\gamma^2 - 1} + \eta\cos^{-1}\frac{1}{\gamma\sqrt{1-\alpha_0}} - 2\gamma^{1/2}\frac{\omega_{b0}}{\omega} \qquad (2)$$

Here A_0 is the electric field amplitude, v_{xA} is the on axis velocity of electrons, $k=(\omega/c)\eta$ is the wave number, $\omega_{b0}=\omega_b\sqrt{\gamma}$ represents the bounce frequency of the oscillation,

$$\eta = (1-\omega_p^2/\omega^2(1+a_0^2/2)^{-1/2})^{1/2}$$

is the ratio of group velocity of the laser in plasma to that in vacuum. $P = a_0 v_{xA}/2c$ $\quad C_1 = F(\gamma_0) + P\sin\phi_0$ is the integration constant, γ_0 is the initial energy of electrons, ϕ_0 is the initial phase of the wave seen by electron, and $\alpha_0 = v_{xA}^2/2c^2$ The separatrix (γ vs ϕ) is given by

$$F(\gamma) - F_{\min} = P(1-\sin\phi) \qquad (3)$$

where, F_{min} is the minimum value of $F(\gamma)$.

4.3 Hybrid acceleration (wakefield + DLA)

Recently, in the regime of $L\geq\lambda_p$, dominance of both wakefield and DLA i.e. hybrid acceleration mechanism have been suggested in mixed gas-jet target ($He+N_2$) [7]. Renewed interest in hybrid regime of acceleration was due to the fact that DLA can double the electron energy in a LWFA and can even have lower energy spread.

4.4 Injection mechanisms in LPA

In LWFA, self-injection of electrons into the wake occur through wave-breaking mechanism [30], which being a highly non-linear process, leads to unstable beam generation with poor beam qualities. Among various other injection schemes, ionization induced injection mechanism [31] using mixed gas (e.g. He + few percent of high-Z gases) and high-Z gas (e.g. N_2, Ar etc.) targets has gained significant interest as it allows to operate the accelerator at comparatively lower density and intensity thresholds. Also, ionization of inner shell electrons of the high-Z gas at the peak of the laser pulse leads to injection in the centre of bubble (wakefield) and also has been found favourable for DLA.

5. Experimental results

Experiments were performed on generation of relativistic electron beams covering $L\sim\lambda_p$ to $L>>\lambda_p$ regimes and conditions suitable for applicability of different acceleration mechanisms were explored. Generation of collimated, directional electron beams was observed. Typical electron beam profiles recorded are shown in Figure T.5.3, showing beam divergence (mrad) varying from several mrad to few tens of mrad.

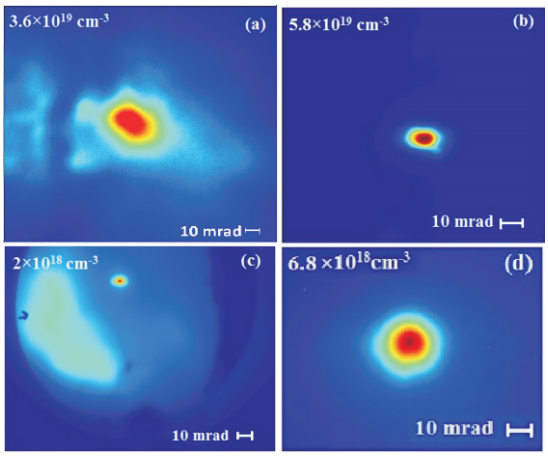

Fig. T.5.3: Typical electron beam profiles, gas jet length: 1.2 mm, (a) He, 200 fs, a_0=1: div. ~30 mrad (b) He, 55 fs, a_0=1.5: div. ~16 mrad, and for gas jet length: 4 mm, (c) N_2+50% He, 60 fs, a_0=4.5: div. ~ 8 mrad and (d) He, 100 fs, a_0=3.5: div. ~11.5 mrad.

5.1 Generation of high-energy, quasi-monoenergetic electron beams

Generation of relativistic electron beams through LPA was studied in a variety of laser and plasma conditions using 1.2 mm and 4 mm gas-jet targets. By varying various parameters, optimum conditions for generation of stable, quasi-monoenergetic electron beams were identified. This also leads to observation of high-energy (>500 MeV) electron beams using 4 mm gas-jet target. Figure T.5.4, T.5.5 & T.5.6 show the generation of stable and reproducible quasi-thermal and quasi-monoenergetic electron spectra with energy spread in the range of 10-20% and maximum energies of ~30 to >500 MeV in various experimental conditions.

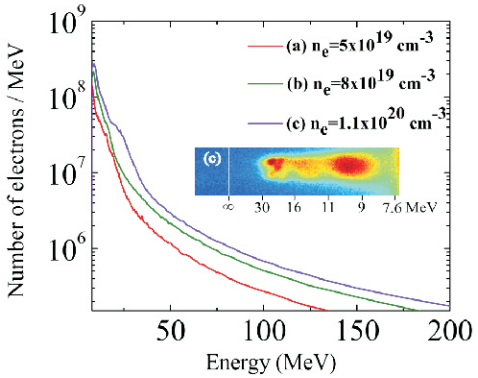

Fig. T.5.4: Typical quasi-thermal electron beam spectra for He gas-jet target of 1.2 mm length:τ~200 fs, E_{max}:~30 MeV: n_e:1.1x10^{20} cm^{-3}, a_0=1.

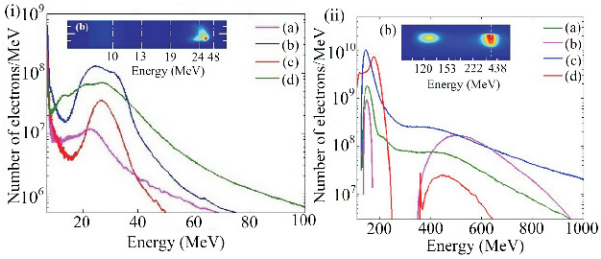

Fig. T.5.5: Typical quasi-monoenergetic spectra for He gas-jet target (i) 1.2 mm length, τ~55 fs, E_{peak}:~28 MeV: n_e:5.8x10^{19} cm^{-3}, a_0=1.5; (ii) 4 mm length, τ~100 fs, E_{peak}:~500 MeV: n_e:6.8x10^{18} cm^{-3}, a_0=3.2.

5.2 Relativistic self-focusing and guiding of laser pulse

Side imaging (Figure T.5.7a) and shadowgram of the laser created channel inside plasma (Figure T.5.7b & c) shows laser interaction length with plasma varying from 0.5 to 4 mm. Relativistic self-focusing and guiding of laser pulse was observed in He gas-jet target (Figure T.5.7a & b) whereas, ionization induced defocusing was observed for high Z (N_2) gas targets (Figure T.5.7c).

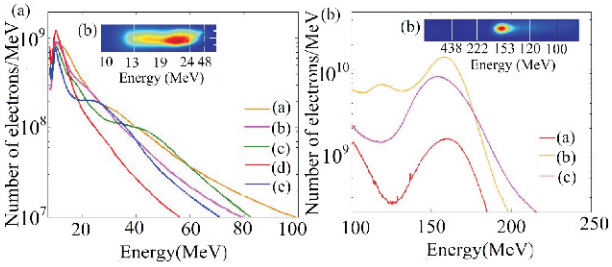

Fig. T.5.6: (a) Typical broad electron beam spectra for N_2 gas-jet target of 1.2 mm length, E_{max} ~55 MeV: n_e: 2x10^{19} cm^{-3}, τ= 60 fs, a_0=1.5. (b) Typical quasi-monoenergetic electron beam spectra for mixed gas-jet target of N_2+50%He of 4 mm length, E_{peak}~168 MeV: n_e: 2x10^{18} cm^{-3},τ=60 fs, a_0=4.5.

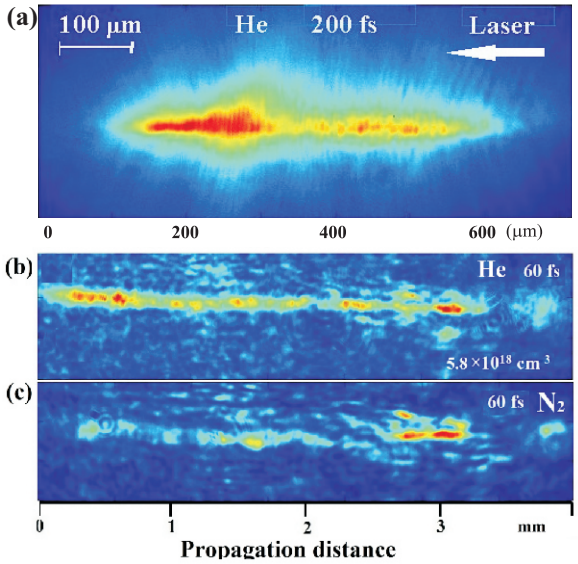

Fig. T.5.7: Typical laser created channels recorded from (a) 90^o Thomson scattering in He gas-jet target of 1.2 mm length: τ=200 fs, n_e=8x10^{19} cm^{-3}, a_0=1. Shadowgram of 4 mm plasma in (b) in He gas-jet target: τ=60 fs, n_e=5.8x10^{18} cm^{-3}, a_0=4.2; (c) in N_2 gas-jet target: τ=60 fs, n_e=1.5x10^{18} cm^{-3}, a_0=4.2.

6. Discussions: theoretical analysis and PIC simulations

Initial investigations were performed in He gas-jet target with long laser pulse duration of 200 fs (L>>λ_p), where generation of quasi-thermal electron beams were observed with maximum energy ~30 MeV with increase of energy with plasma density (Figure T.5.4) which is higher than that

estimated from wakefield (~5 MeV), suggesting DLA could be dominant over SM-LWFA [17]. However, on reducing the laser pulse duration to ~55 fs ($L>_p$), wakefield contribution was found to strengthen as we observed generation of quasi-monoenergetic electron beams (Figure T.5.5i). Since laser pulse is still long, contribution of DLA could not be neglected, and hence, hybrid acceleration was identified as the dominant mechanism [18]. In another experiment, with 100 fs laser pulse, hybrid regime of acceleration in He has demonstrated acceleration of electrons to >500 MeV (Figure T.5.5ii) [20]. Generation of electron beams were also studied in a density range below the self-injection threshold with the assistance of ionization induced injection using mixed ($He+N_2$) and N_2 gas-jet targets. Interestingly, a pure DLA acceleration in short laser pulse duration of ~55 fs was identified, however, electron beams with maximum energy of ~55-60 MeV and broad spectra were observed (Figure T.5.6a) [18]. Hence, in another experiment [19] ($L\sim\lambda_p$) in high-Z N_2 and mixed gas targets, through optimization of electron beam properties interestingly, we could observe generation of stable and reproducible quasi-monoenergetic electron beams (average energy spread of ~21%) with average peak energy of ~168 MeV from an optimum gas mixture of $He+50\%N_2$ (Figure T.5.6) in a pure DLA regime. Such interesting observations, in different parametric regimes and applicable acceleration mechanisms, were demonstrated for the first time.

6.1 Theoretical analysis

The maximum energy gain of electrons through DLA was estimated using the formalism in Eq. 1-3. The largest value of the right hand side of Eq. (3) is 2P. Therefore, a horizontal line was drawn in Figure T.5.8a at a height of 2P from F_{min}, which cuts the F(γ) curve at two points R and S corresponds to the bottom and top of the separatrix (Figure T.5.8b) respectively. The cross points of the separatrix occur at $\gamma=\gamma_{opt}$, which is the optimum energy required for electrons to get trapped in the laser field. Figure T.5.8a and T.5.8b show that the maximum energy acquired by a trapped electron is ~34 MeV (γ~67.5), close to the energy of ~30 MeV observed in the experiment (Figure T.5.4b). The total energy gain from wakefield and DLA was compared with the experimentally observed values over the density regime in case of short laser pulse duration of ~55 fs, good agreement of which shows the dominance of pure DLA and hybrid regime of acceleration (Figure T.5.9).

The theoretical model was further extended to estimate the dephasing length of electrons in the laser field for which coupled differential equations were derived and plotted in Figure T.5.10. The dephasing length was estimated to be 100 - 200 μm.

Further, rate of dephasing of electrons (R) in case of DLA was also derived to study its dependence on plasma density [19].

$$\frac{d\phi}{d\xi}=\frac{1-\omega_{b0}/\omega\gamma^{\frac{1}{2}}}{\left(1-\alpha_0-1/\gamma^2\right)^{\frac{1}{2}}}-\eta,\ \frac{d\gamma}{d\xi}=-\frac{a_0\left(\alpha_0/2\right)^{\frac{1}{2}}}{\left(1-\alpha_0-1/\gamma^2\right)^{\frac{1}{2}}}\cos\phi \quad (4)$$

$$R=-\gamma\left[\frac{1-\omega_{b0}/\omega\sqrt{\gamma}}{(1-\alpha_0-1/\gamma^2)^{1/2}}-\eta\right] \quad (5)$$

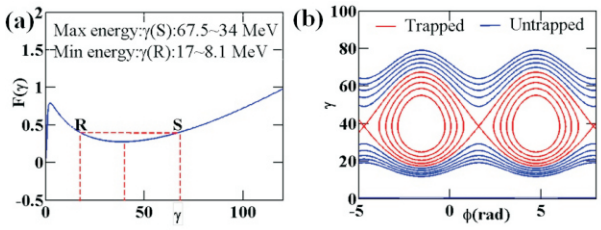

Fig. T.5.8: (a) Plot of F(γ) vs γ; (b) Separatrix (γ vs ϕ) plot. η = 0.983 (average value for the density range used), a_0=1.

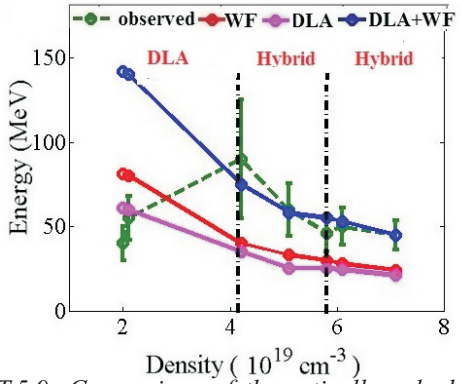

Fig. T.5.9: Comparison of theoretically calculated energy with experimentally observed value.

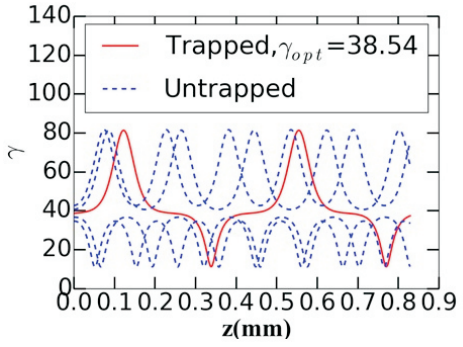

Fig. T.5.10: (a) Plot of γ vs z; η = 0.983 (average value for the density range used), a_0=1.

6.2. 2D PIC simulation results

2D PIC simulations were performed using code EPOCH [32] and OSIRIS [33] and were found to be in good agreement with experiments. Results of 2D EPOCH simulations performed in He plasma ($L>>\lambda_p$) shows clear channel formation (Figure T.5.11) suggesting pure DLA acceleration. At shorter laser pulse duration, formation of bubble was observed (Figure T.5.12a) signifying strengthening of wakefield and betatron oscillation of bunch of self-injected electrons inside the bubble structure signifies energy gain by DLA also i.e. hybrid acceleration. This is also confirmed from Figure T.5.12b where we have estimated the separate contribution of wakefield (γ_x) and DLA (γ_y) to the total energy gain, given by:

$$\gamma_y = -\int_0^t \frac{2ePE_y}{(mc)^2} dt, \gamma_x = -\int_0^t \frac{2ePE_x}{(mc)^2} dt$$

where E_y, P_y and E_x, P_x are transverse and longitudinal electric field and momentum respectively. Similar hybrid acceleration with maximum energy of 500-600 MeV is observed using code OSIRIS with 100 fs (Figure T.5.12 c & d). This is consistent with experimental observation of Figure T.5.5i & ii.

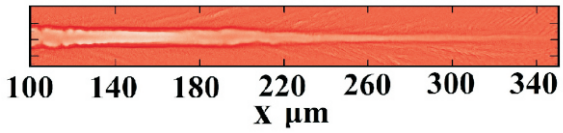

Fig. T.5.11: EPOCH: Electron density plot along laser propagation direction: $n_e=7x10^{19}$ cm^{-3}, $\tau=200$ fs, $a_0=1$.

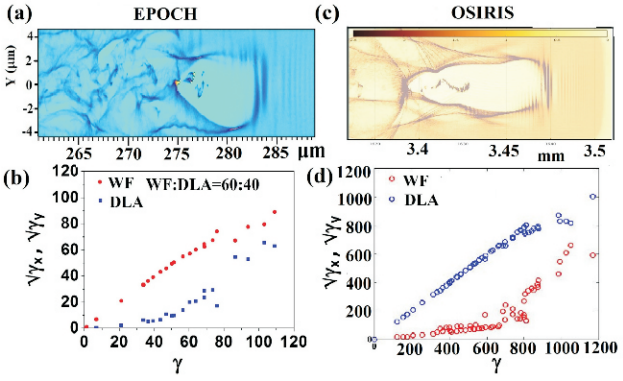

Fig. T.5.12: Electron density plot and corresponding energy contributions separately from DLA and wakefield of He at $n_e=5.8x10^{19}$ cm^{-3}, $\tau=55$ fs, $a_0=1.5$, plasma length=1mm using EPOCH (a & b), and $n_e=6.8x10^{18}$ cm^{-3}, $\tau=100$ fs, $a_0=3.5$, plasma length=4 mm using OSIRIS (c & d).

A pure DLA regime was also identified in N_2 (Figure T.5.13a & b) and high Z N_2+50%He plasma target (Figure T.5.13c & d) with quasi-monoenergetic electron beams (Figure T.5.13 d). The results are consistent with that observed in Figure T.5.6a & b.

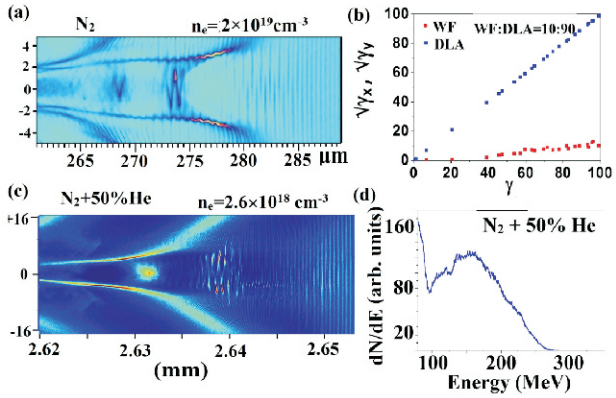

Fig. T.5.13: EPOCH: (a) Electron density plot and (b) corresponding separate contribution of N_2 at $n_e=2x10^{19}$ cm^{-3}: $\tau=55$ fs, $a_0=1$. Plasma length=1 mm and (c) N_2+50%He at $n_e=2.6x10^{18}$ cm^{-3}, $\tau=60$ fs, $a_0=4$. Plasma length=4 mm (d) corresponding energy spectra.

7. Relativistic electron beam radiography using LPA

LPA is now being considered for various potential applications, e.g. as a compact electron injector for a conventional accelerator, generation of synchrotron radiation, and radiography, interrogation of dense objects, and radiotherapy. In the present investigation also, radiography applications of relativistic electron beams generated from the laser plasma interactions with Ar and He gas-jet targets was explored [21]. Electron beams with large divergence and broad spectrum with maximum energy of 50 MeV were observed from Ar gas target whereas collimated electron beams with quasi-monoenergetic spectra with peak electron of ~150 MeV were observed from He gas target.

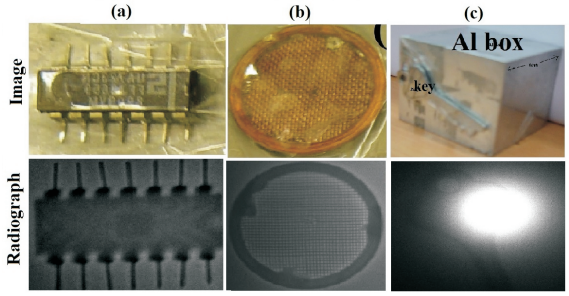

Fig. T.5.14: Images of samples and radiographs of (a) IC chip, (b) Cu mesh using Ar electron beams and (c) Key kept behind an Al block with He electron beams.

GEANT4 Monte Carlo simulations were performed to reconstruct the radiographic images and were found to be consistent with the experimental results. Images of different samples and corresponding radiographs are shown in Figure T.5.14. Effects of two different electron beams on radiographs were studied (Figure T.5.15a & b) and verified with GEANT4 simulations through reconstruction of the images (Figure T.5.15c). Minimum resolution of ~75 μm was achieved (Figure T.5.15d).

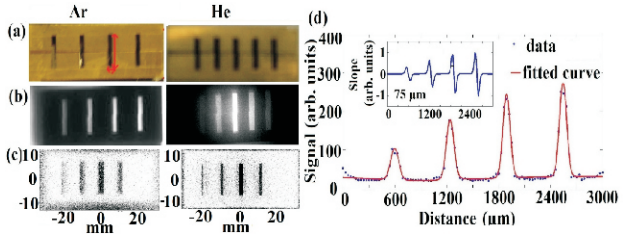

Fig. T.5.15: Images and radiographs of 5 cm thick brass groove: (a) Samples, (b) Corresponding radiographs, (c) GEANT4 reconstructed image and (d) Estimation of resolution of radiograph (b) recorded using Ar electron beams.

Further, radiographs of some biological plant samples were recorded (Figure T.5.16a & b), showing finer veins of the leaves used. Finally, suitability of LPA for radiotherapy applications was explored, by estimating energy deposition in adipose tissue (Figure T.5.16c) through GEANT4 simulations.

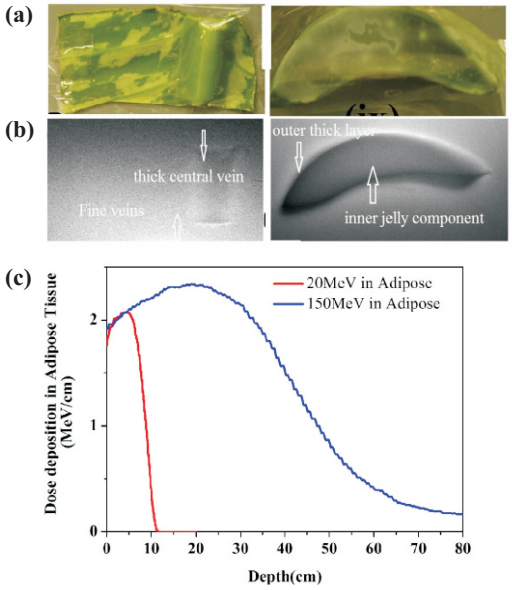

Fig. T.5.16: Images and radiographs of biological plant samples of a thick leaf and cross-section of aloe-vera: (a) samples. (b) radiographs, (c) Estimation of penetration of electron beams in adipose tissue.

8. Future perspective and use of PW laser

It has been now more than one and half decade since the first demonstration of possibility of generation of quasi-monoenergetic electron beams through LPA. Subsequently, it was realised that stable, and high-quality electron beams could be obtained through LPA, by precise tuning of the laser and plasma parameters, and acceleration length. Based on that, generation of sub-GeV and more than GeV electron beams have been demonstrated in various laboratories across the world. Most of the earlier investigations were performed using 100 TW class laser systems, and now investigations are being performed using PW class laser systems [34]. Recently, using a PW laser system, acceleration of electrons to 8 GeV energy has been demonstrated at BNL, USA [8]. At the same time suitability of LPA for generation of intense x-ray/γ-ray radiation using various techniques and for other applications has also been investigated.

In nutshell, during last decade, worldwide efforts have led to generation of high-quality, quasi-monoenergetic electron beams of energy up to several GeV level using LPA. In future, large accelerators (colliders) may also be based on plasma acceleration technique. Further advancement in the field of laser technology, facilitating availability of ultra-short laser systems with high peak and average power (repetition rate of tens of kHz), would provide impetus to the practical applications of LPA.

At RRCAT also, initial investigations were performed using 10 TW laser, followed by recent results shown in this article with 150 TW laser system. A 1 PW, 25 fs, Ti:sapphire laser system (Figure T.5.17) is under installation at RRCAT, and shall be used to perform further investigations with longer (≥10 mm) plasma targets to generate GeV and higher energy electron beams.

Fig. T.5.17: 1 PW, 25 fs, Ti:sapphire laser system under installation at RRCAT.

9. Conclusion

We have performed detailed investigation on generation of relativistic electron beams from Laser Plasma Accelerator (LPA). Stable, reproducible generation of quasi-monoenergetic electron beams from few tens of MeV to >500 MeV energy was observed with varying laser and plasma parameters. In addition, various physical aspects of the laser plasma interaction and LPA were also investigated, particularly role of different acceleration mechanisms was identified. Further, radiography application was explored along with suitability of LPA in radiotherapy applications.

Studies performed at RRCAT, using 150 TW laser, and further investigations planned using 1 PW laser, would be of significance for development of compact, and comparatively low cost electron accelerator, and also laser synchrotron radiation source providing intense, ultra-short (fs regime), tunable x-ray/γ-ray radiation for various possible applications.

Acknowledgments

The research investigation presented here is part of the Ph. D. Thesis work of first author of this article, Ms. Dipanjana Hazra, Senior Reseacrh Fellow, Homi Bhabha National Institute (HBNI). Research work was performed under the guidance of Prof. Anand Moorti, SO-H, Head, Advanced Plasma Acceleration Section, Laser Plasma Division, RRCAT, Indore. The thesis has been submitted to HBNI, RRCAT, Indore.

Authors acknowledge contributions of all towards this research work. We thank Dr. J. A. Chakera, Head, Laser Plasma Division, for his support and contributions. We acknowledge contributions of Shikha Mishra through her participation in the experiments, data analysis, and GEANT4 simulations, Dr. Ajit Upadhyay for EPOCH and Dr. Mithun Karmakar, Dr. Bhabesh Patel, and Prof. S. Sengupta from IPR, Gandhinagar, for OSIRIS PIC simulation. We thank Dr. B. S. Rao for his association in initial experimental investigation.

We are thankful to R. A. Khan, and A. Singla for the 150 TW Ti:sapphire laser operation and characterization, and D. Karmakar for help in setting up the experiment. Contributions of R. P. Kushwaha, S. Sebastin, L. Kisku, K. C. Parmar, Sunil Meena and P. K. Tripathy for providing mechanical / workshop support, and of other LPD members are also acknowledged.

It is a pleasure to thank Shri S. V. Nakhe, Director, Laser Group and Materials Science Group, RRCAT, and Shri. Debashis Das, Director, RRCAT, for their keen interest and continuous support.

References

[1] Waldemar Scharf, "Particle Accelerators and their uses", Harwood Academic Publishers, (1986).

[2] E. Esarey *et al*., Rev. Mod. Phys., 81, 1229 (2009).

[3] S. M. Hooker, "Developments in laser-driven plasma accelerators", Nature Photonics, 7, 775 (2013).

[4] P. Gibbon, Short Pulse Laser Interactions with Matter: An Introduction (Imperial College Press, London, 2005).

[5] T. Tajima *et al*., "Laser electron accelerator", Phys. Rev. Lett., 43, 268 (1979).

[6] A. Pukhov *et al*., "Particle acceleration in relativistic laser channels", Phys. Plasmas, 6, 2847 (1999).

[7] J. L. Shaw *et al*., "Role of Direct Laser Acceleration of Electrons in a Laser Wakefield Accelerator with Ionization Injection", Phys. Rev. Lett., 118, 064801 (2017).

[8] A. J. Gonsalves *et al.* "Petawatt Laser Guiding and Electron Beam Acceleration to 8 GeV in a Laser-Heated Capillary Discharge Waveguide", Phys. Rev. Lett., 122, 084801 (2019).

[9] C. Gahn *et al.,* "Multi-MeV Electron Beam Generation by Direct Laser Acceleration in High-Density Plasma Channels.", Phys. Rev. Lett., 83, 4772 (1999).

[10] A. Moorti, and B. S. Rao, "Laser Wakefield Acceleration: An advanced technique for compact electron accelerators", Theme Article, RRCAT Newsletter, vol.26, Issue 2 (2013).

[11] A. Moorti, "Ultraintense Laser Plasma Interaction: Physics and Applications", Kiran: Bulletin of the Indian Laser Association, Special issue on International year of Light-2015, vol.26, No.2, pp.19 (2015).

[12] A. Moorti and P. A. Naik, Laser Wake-field Electron Acceleration: An Advanced Technique for Development of Compact Accelerators and Radiation Sources, Physics News, Bulletin of the Indian Physics Association, vol.48, No. 3, July-September, (2018).

[13] B. S. Rao, A. Moorti, P. A. Naik, and P. D. Gupta, "Effect of chirp on self-modulation and laser wake-field electron acceleration in the regime of quasi-monoenergetic electron beam generation", Phys. Rev. Spec. Topics Accel. Beams, 16, 091301 (2013).

[14] B. S. Rao, A. Moorti, R. Rathore, J. A. Chakera, P. A. Naik, and P. D. Gupta, "High-quality stable electron beams from laser wake-field acceleration in high

density plasma", Phys. Rev. Spec. Topics-Accel. Beams, 17, 011301 (2014).

[15] B. S. Rao, A. Moorti, J. A. Chakera, P. A. Naik, and P. D. Gupta, Quasi-monoenergetic electron beams from a few-terawatt laser driven plasma acceleration using a nitrogen gas jet, Plasma Phys. Control. Fusion, 59, 065006 (2017).

[16] B. S. Rao A. Moorti, R. Rathore, J. A. Chakera, P. A. Naik, and P. D. Gupta, "High quality electron beam from laser wake-field acceleration in a solid plasma plume target", Appl. Phys. Lett., 102, 231108 (2013).

[17] D. Hazra, A. Moorti, B. S. Rao, A. Upadhayay, J. A. Chakera, and P. A. Naik, "Betatron resonance electron acceleration and generation of quasi-monoenergetic electron beams using 200fs Ti:Sa laser pulses", Plasma Phys. Controlled Fusion, 60, 085015 (2018).

[18] D. Hazra, A. Moorti, A. Upadhayay, and J. A. Chakera, "Determination of hybrid and direct laser acceleration dominated regimes in a 55fs laser driven plasma accelerator with ionization induced injection", Under review in Phys. Review Accelerators and Beams, arXiv:1902.01203v2 [physics.plasm-ph].

[19] D. Hazra, A. Moorti, S. Mishra, A. Upadhyay, and J. A. Chakera, "Direct laser acceleration of electrons in high-Z gas target and effect of threshold plasma density on electron beam generation", Plasma Physics and Controlled Fusion, 61, 125016 (2019).

[20] D. Hazra, A. Moorti, *et al*., "An experimental study on high-energy electron acceleration in He gas-jet target and effect of laser pulse duration", Manuscript under preparation.

[21] D. Hazra, S. Mishra, A. Moorti, and J. A. Chakera, "Electron radiography with different beam parameters using laser plasma accelerator", Physical Review Accelerators and Beams, 22, 074701 (2019).

[22] D. Strickland and G. Mourou, Opt. Comm., 56, 219 (1985).

[23] S. Mishra, D. Hazra, A. Moorti, and J. A. Chakera, "An experimental and GEANT4 simulation study on design of a broad energy-range magnetic spectrograph for laser plasma accelerator", JINST, 15, P01034 (2020).

[24] C. E. Max *et al*., "Self-modulation and self-focusing of electromagnetic waves in plasmas", Phys. Rev. Lett., 33, 209, (1974).

[25] A. Modena *et al*., "Electron acceleration from the breaking of relativistic plasma waves", Nature (London) 377, 606 (1995).

[26] B. Hidding *et al., "*Generation of Quasimonoenergetic Electron Bunches with 80-fs Laser Pulses", Phys. Rev. Lett., 96, 105004 (2006);

[27] A. Pukhov *et al*, "Phenomenological theory of laser-plasma interaction in "bubble" regime", Appl. Phys. B: Lasers Opt.74, 355 (2002).

[28] W. Lu *et al.,* "Generating multi-GeV electron bunches using single stage laser wakefield acceleration in a 3D nonlinear regime", Phys. Rev. ST Accel. Beams, 10, 061301 (2007).

[29] G. D. Tsakiris *et al*., "Laser induced electron acceleration in the presence of static electric and magnetic fields in a plasma", Phys. Plasmas, 7 3017 (2000).

[30] S.V. Bulanov *et al*.,"Transverse wake wave breaking", Phys. Rev. Lett., 78, 4205 (1997).

[31] A. Pak *et al*., "Injection and Trapping of Tunnel-Ionized Electrons into Laser-Produced Wake", Phys. Rev. Lett.,104, 025003 (2010).

[32] T D Arber *et al*., Contemporary particle-in-cell approach to laser-plasma modelling, Plasma Phys. Control. Fusion, 57, 1113001 (2015).

[33] Lecture Notes in Computer Science: Computation Science–ICCS 2002, R. A. Fonseca et al., edited by P. M. A. Sloot *et al*., Berlin: Springer, 2331, 342 (2002).

[34] C. N. Danson *et al*., Petawatt and exawatt class lasers worldwide, High Power Laser Science and Engineering, 7, e54 (2019).